

Impact of Fission Products Impurity on the Plutonium Content of Metal- and Oxide- Fuels in Sodium Cooled Fast Reactors

Hikaru Hiruta
Gilles Youinou

September 2013



The INL is a U.S. Department of Energy National Laboratory
operated by Battelle Energy Alliance

DISCLAIMER

This information was prepared as an account of work sponsored by an agency of the U.S. Government. Neither the U.S. Government nor any agency thereof, nor any of their employees, makes any warranty, expressed or implied, or assumes any legal liability or responsibility for the accuracy, completeness, or usefulness, of any information, apparatus, product, or process disclosed, or represents that its use would not infringe privately owned rights. References herein to any specific commercial product, process, or service by trade name, trade mark, manufacturer, or otherwise, does not necessarily constitute or imply its endorsement, recommendation, or favoring by the U.S. Government or any agency thereof. The views and opinions of authors expressed herein do not necessarily state or reflect those of the U.S. Government or any agency thereof.

Impact of Fission Products Impurity on the Plutonium Content of Metal- and Oxide- Fuels in Sodium Cooled Fast Reactors

**Hikaru Hiruta
Gilles Youinou**

September 2013

**Idaho National Laboratory
Reactor Physics Analysis & Design Department
Idaho Falls, Idaho 83415**

**Prepared for the
U.S. Department of Energy
Office of Nuclear Energy
Under U.S. Department of Energy-Idaho Operations Office
Contract DE-AC07-05ID14517**

CONTENTS

1.	Introduction.....	1
2.	Modeling and Calculation Method.....	3
3.	Results and Discussions.....	5
4.	Summary.....	6
5.	References.....	7

FIGURES

Figure 1.	TRITON quarter-assembly models of metal- and oxide-fuel assemblies.	4
Figure 2.	Pu enrichments as a function of FP losses for the metal-fuel assembly.	5
Figure 3.	Pu enrichments as a function of FP losses for the oxide-fuel assembly.	6

TABLES

Table 1.	Pu and FP present in the reference 51 GWd/TIHM UOX SNF (10-year cooling time)	1
Table 2.	Composition of the Pu^{FP} mixture as a function of the FP losses during the reprocessing of UOX SNF.....	2
Table 3.	Assembly dimensions and other physical data for SFR assembly modeling.....	3
Table 4.	Pu enrichments as a function of FP losses for the metal-fuel assembly.....	5
Table 5.	Pu enrichments as a function of FP losses for the oxide-fuel assembly.....	6

FUEL CYCLE OPTIONS CAMPAIGN

IMPACT OF FISSION PRODUCTS IMPURITY ON THE PLUTONIUM CONTENT OF METAL- AND OXIDE- FUEL IN SODIUM COOLED FAST REACTORS

1. Introduction

This short report presents the neutronic analysis to evaluate the impact of fission product impurity on the Pu content of Sodium-cooled Fast Reactor (SFR) metal- and oxide- fuel fabrication. The similar work has been previously done for PWR MOX fuel [1]. The analysis will be performed based on the assumption that the separation of the fission products (FP) during the reprocessing of UOX spent nuclear fuel assemblies is not perfect and that, consequently, a certain amount of FP goes into the Pu stream used to fabricate SFR fuels. Only non-gaseous FPs have been considered (see the list of 176 isotopes considered in the calculations in Appendix 1 of Reference 1). Throughout of this report, we define the mixture of Pu and FPs as Pu^{FP} .

The main objective of this analysis is to quantify the increase of the Pu content of SFR fuels necessary to maintain the same average burnup at discharge independently of the amount of FP in the Pu stream, i.e. independently of the Pu^{FP} composition. The FP losses are considered element-independent, i.e., for example, 1% of FP losses mean that 1% of all non-gaseous FP leak into the Pu stream.

The amount of Pu and FP present in the reference 51 GWd/TIHM UOX SNF (4.3% U-235) after 10 years of cooling time is given in Table 1 below. It shows that 1 ton of UOX SNF contains 11.33 kg of Pu and 44.05 kg of non-gaseous FP, hence, for example, if the FP losses are equal to 1 wt%, the Pu^{FP} mixture contains 11.33 kg of Pu and 0.4405 kg of non-gaseous FP, or put in differently, $Pu^{FP}-1\% = 96.26$ wt% Pu + 3.74 wt% FP. The compositions of the Pu^{FP} mixture as a function of the FP losses during the reprocessing of UOX SNF are presented in Table 2. After the Pu (or Pu^{FP}) has been separated, an additional 1-year decay period is also taken into account before the MOX fuel is actually loaded in the reactor in order to allow for transportation and fuel fabrication. During this 1-year about 5% of the ^{241}Pu decays on ^{241}Am .

The rest of this report is organized as followings. Section 2 explains in detail the computational method and modeling used for the analysis. Section 3 talks about results (i.e., Pu enrichment as a function of FP loss) of calculations. Finally Section 4 summarizes the report.

Table 1. Pu and FP present in the reference 51 GWd/TIHM UOX SNF (10-year cooling time)

Isotope	kg/TIHM
Pu238	0.295
Pu239	6.153
Pu240	2.930
Pu241	1.086
Pu242	0.864
Total Pu	11.33
ToTal FP	52.64
Total FP (non-gas)	44.05
RatioFP/Pu	4.646
Ratio FP _{non-gas} /Pu	3.888

Table 2. Composition of the Pu^{FP} mixture as a function of the FP losses during the reprocessing of UOX
SNF

FP losses [wt%]	FP in the Pu^{FP} mixture [wt%]	Pu in the Pu^{FP} mixture [wt%]
0.25	0.96	99.04
0.50	1.91	98.09
0.75	2.83	97.17
1.00	3.74	96.26
2.00	7.22	92.78
3.00	10.45	89.55
4.00	13.46	86.54
5.00	16.28	83.72

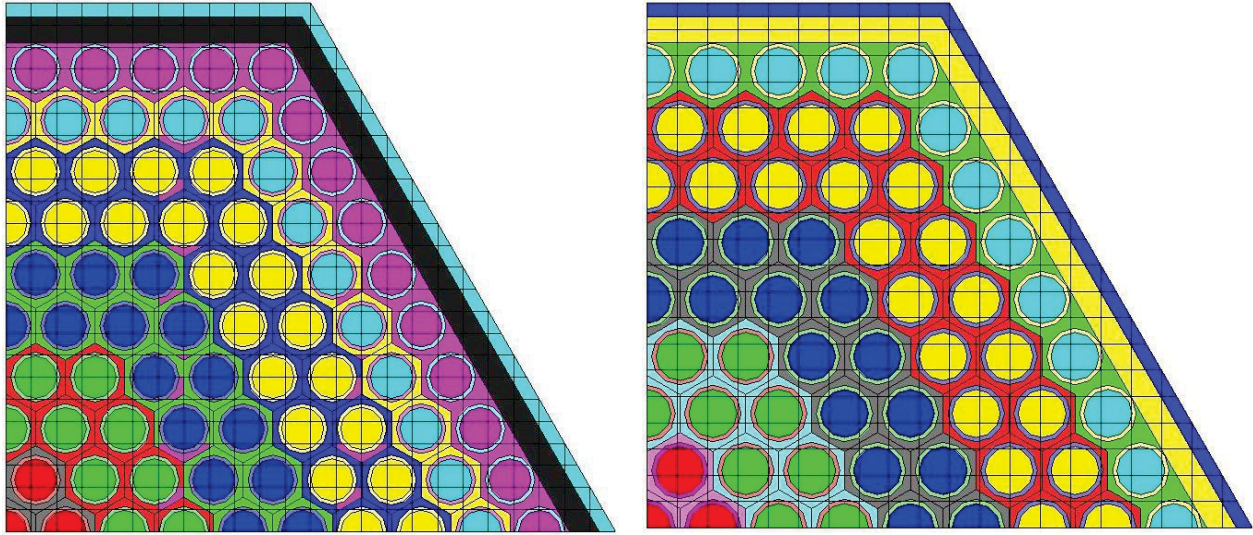
2. Modeling and Calculation Method

SCALE6.1.2 [2] code system has been selected to perform all calculations because of its capability to handle several types of reactor physics and criticality safety simulations including lattice physics calculations. NEWT, which is the 2D discrete ordinates solver in non-orthogonal geometries, has a capability to model heterogeneous assembly geometry by closely approximating curved geometries. TRITON module, which effectively couples NEWT with ORIGEN depletion module, performs burnup calculations together with the automated cross section processing such as resonance self-shielding calculations by BONAMI (unresolved range) and CENTRM (resolved range) at each depletion sub-interval. The 238-group ENDF/B-VII.1 library has been used for these calculations.

The assembly dimensions and other physical data for the fuel are determined based on S-PRISM and ABR designs in References 3 and 4. These data are presented in Table 3. Figure 1 shows the plot of modeled geometries for both assemblies. The color of each fuel-pin cell represents the burnup zoning. Instead of modeling the gap between fuel pellet surface and clad inner surface, the fuel is smeared into the gap region, and its density is multiplied by the volume ratio. Only a quarter of each assembly is modeled by applying the reflective boundary condition at each orthogonal surface (top, bottom, and left) and white boundary condition at the non-orthogonal surface (right). The unstructured version of Coarse-Mesh Finite-Difference (CMFD) method is applied in order to accelerate the convergence of inner iterations. The thermal iteration is turned off since negligible contribution from thermal energy groups is expected in both fast reactor assemblies. The product quadrature set is assigned to have six directions per quadrant (2 polar \times 3 azimuthal angles).

Table 3. Assembly dimensions and other physical data for SFR assembly modeling.

	Metal-Fueled Assembly	Oxide-Fueled Assembly
Number of Fuel Pins	271	217
Fuel-Pin Inner Diameter [cm]	0.6322	0.724
Fuel-Pin Outer Diameter [cm]	0.744	0.851
Fuel-Pin Pitch [cm]	0.90687	1.01356
P/D	1.21891	1.19102
Assembly Pitch [cm]	16.1417	16.1417
Duct Gap [cm]	0.4318	0.4318
Duct Wall Thickness [cm]	0.3937	0.3937
Fuel Density [g/cm ³]	15.05	11.05
Smeared Fuel Density [g/cm ³]	11.30	10.50
Clad (HT9) Density [g/cm ³]	7.894	7.894
Coolant (Na) Density [g/cm ³]	0.8136	0.8136
Average Discharge Burnup [GWd/t]	73	102.6
Specific Power [W/g]	42.5	30.4
EFPD [days]	1717.6	3375
Fuel Temperature [°K]	885.33	1196
Clad (HT9) Temperature [°K]	793.82	795.3
Coolant Temperature [°K]	793.82	795.3
Reference Pu Enrichment [wt%]	13.4	17.2



(a) Metal-Fuel Assembly Model

(b) Oxide-Fuel Assembly Model

Figure 1. TRITON quarter-assembly models of metal- and oxide-fuel assemblies.

All models take into account 1 year of aging after the fuel fabrication. The 3-batch scheme is assumed for both assemblies. This will give the average end-of-cycle (EOC) burnup of 48.7 GWd/t for metal-fuel and 68.4 GWd/t for oxide-fuel assemblies. Calculations based on the reference Pu enrichment in Table 1 without any fission-products show that k_{∞} at average EOC burnup is equal to 1.2020 for metal-fuel and 1.1617 for oxide fuel assemblies. These are the conditions necessary to hold at every time adding fission products into fuel compositions. Therefore, Pu^{FP} (Pu+FP) enrichments are determined by iterative approach in order to obtain the same k_{∞} at the average EOC burnup.

3. Results and Discussions

Calculations have been performed for both metal-fuel and oxide-fuel assemblies shown in Table 3 and Figure 1. The Pu^{FP} enrichments are determined by adjusting them until k_{∞} at the average EOC burnup becomes equal to that of the reference core. Note that there has been a bias observed in our results exhibiting a jump in Pu^{FP} enrichment between 0 wt% and negligibly small amount (say a 10000th of a percentage) of FP losses followed by linear increase of the enrichment, possibly caused by the introduction of a large number of FPs (i.e., 176 FPs). Therefore, this bias has been subtracted from calculated Pu^{FP} enrichments (0.08wt% for the metal-fuel and 0.167 wt% for the oxide fuel assemblies), which is the same treatment made in Reference 1.

Table 4 and Figure 2 show Pu^{FP} and Pu content in the metal-fuel assembly necessary to maintain the same average burnup at discharge of 73 GWd/THM independently of the amount of the FP losses. The same set of results for the oxide-fuel assembly, which has discharge of 102.6 GWd/THM, is presented in Table 5 and Figure 3. By analyzing the slope of each plot, it can be seen that the mass of Pu increases approximately 0.85% per percent of FP losses for the metal-fuel assembly and 1.1% per percent of FP losses for the oxide-fuel assembly. (Note that the Pu content increase in PWR MOX fuel is ~3.5% per percent of FP losses [1]).

Table 4. Pu enrichments as a function of FP losses for the metal-fuel assembly.

FP losses [wt%]	Pu^{FP} enrichment [wt%]	Pu enrichment [wt%]
0.00	13.400	13.400
0.25	13.564	13.433
0.50	13.722	13.460
0.75	13.883	13.489
1.00	14.042	13.516
2.00	14.692	13.632
3.00	15.347	13.744
4.00	16.017	13.860
5.00	16.691	13.974

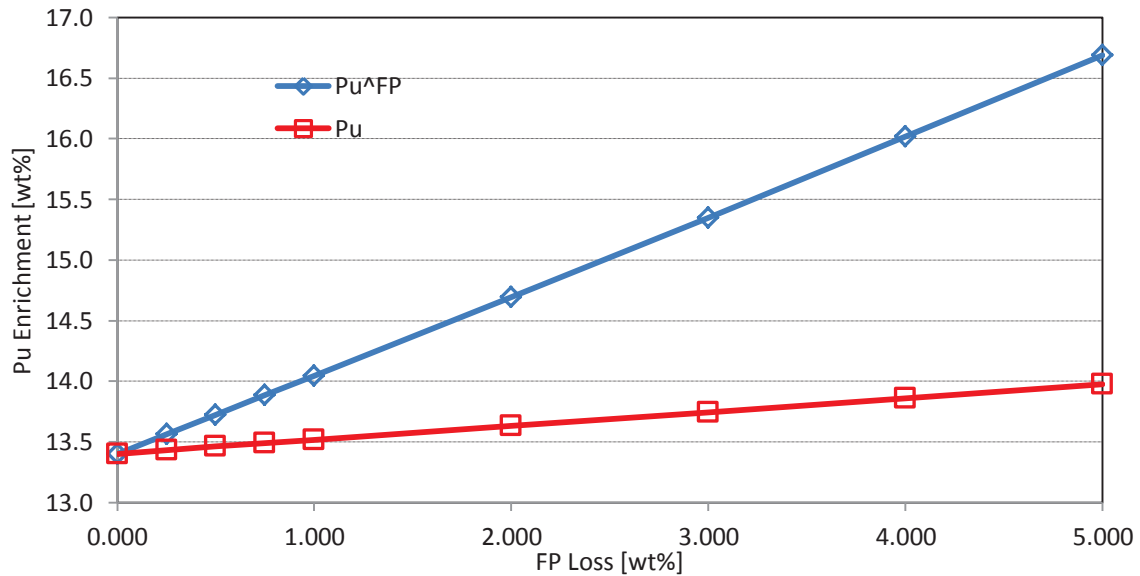


Figure 2. Pu enrichments as a function of FP losses for the metal-fuel assembly.

Table 5. Pu enrichments as a function of FP losses for the oxide-fuel assembly.

FP losses [wt%]	Pu^{FP} enrichment [wt%]	Pu enrichment [wt%]
0.00	17.200	17.200
0.25	17.416	17.249
0.50	17.633	17.297
0.75	17.851	17.345
1.00	18.069	17.393
2.00	18.949	17.582
3.00	19.841	17.768
4.00	20.748	17.955
5.00	21.668	18.141

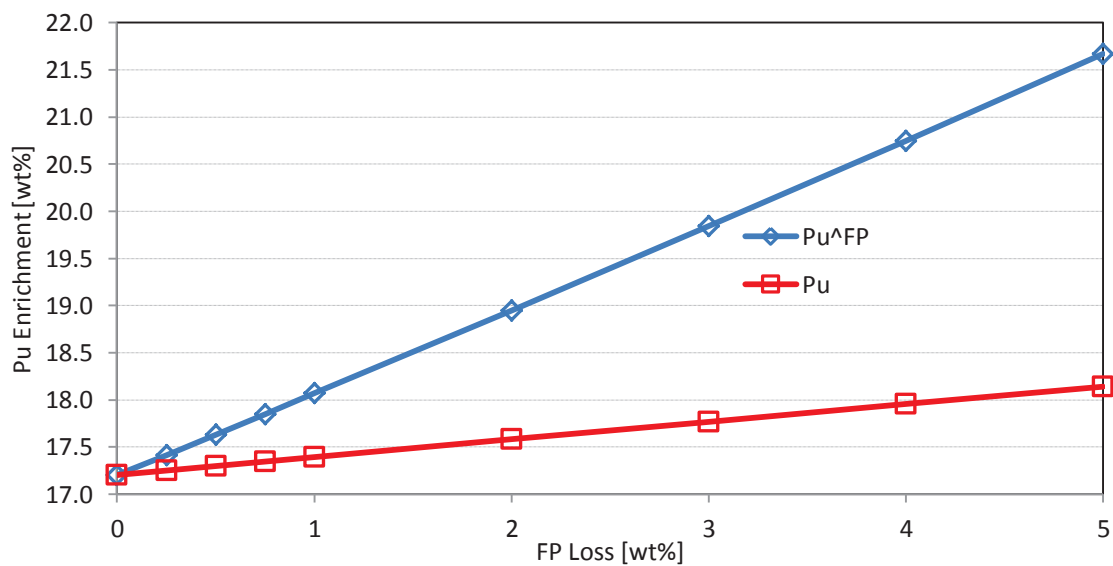


Figure 3. Pu enrichments as a function of FP losses for the oxide-fuel assembly.

4. Summary

This short report presented the neutronic analysis to evaluate the impact of fission product impurity on the Pu content of SFR fuel fabrication. The analysis was performed based on the assumption that the separation of the fission products (FP) during the reprocessing of UOX spent nuclear fuel assemblies is not perfect and that, consequently, a certain amount of FP goes into the Pu stream used to SFR fuels. TRITON module in SCALE6.1.2 was used for this analysis.

The main objective of this analysis was to quantify the increase of the Pu content of SFR fuels necessary to maintain the same average burnup at discharge (73 GWd/THM for metal-fuel assembly and 102.6 GWd/THM for oxide-fuel assembly) independently of the amount of FP in the Pu stream, i.e. independently of the Pu^{FP} composition. The FP losses were considered element-independent, i.e., for example, 1% of FP losses mean that 1% of all non-gaseous FP leak into the Pu stream.

Calculations showed that the Pu content of SFR fuels increased approximately 0.85% per percent of FP losses for the metal-fuel assembly and 1.1% per percent of FP losses for the oxide-fuel assembly. These were significantly less than the Pu content increase in PWR MOX fuel (~3.5% per percent of FP losses).

5. References

1. A. Alfonsi and G. Youinou, "Impact of Fission Products Impurity on the Plutonium Content in PWR MOX Fuels," *INL/EXT-12-26114* (2012).
2. *Scale: A Comprehensive Modeling and Simulation Suite for Nuclear Safety Analysis and Design*, ORNL/TM-2005/39, Version 6.1, June 2011. Available from Radiation Safety Information Computational Center at Oak Ridge National Laboratory as CCC-785.
3. A. E. Dubberley, K. Yoshida, Ce. E. Boardman, and T. Wu, "SuperPRISM Oxide and Metal Fuel Core Designs," *Proc. 8th Int. Conf. Nucl. Eng. (ICONE 8)*, April 2-6, 2000, Baltimore, MD (2000).
4. E. A. Hoffman, W. S. Yang, and R. N. Hill, "Preliminary Core Design Studies for the Advanced Burner Reactor over a Wide Range of Conversion Ratios," *ANL-AFCI-177* (2006).